ISSN 1063-7842, Technical Physics, 2020, Vol. 65, No. 7, pp. 1106–1113. © Pleiades Publishing, Ltd., 2020.
Russian Text © The Author(s), 2020, published in Zhurnal Tekhnicheskoi Fiziki, 2020, Vol. 90, No. 7, pp. 1151–1158.

PHYSICAL SCIENCE OF MATERIALS

# Electrical and Mechanical Properties of the High-Permittivity Ultra-High-Molecular-Weight Polyethylene-Based Composite Modified by Carbon Nanotubes

**I. A. Markevich[a,*], G. E. Selyutin[a], N. A. Drokin[b], and A. G. Selyutin[c]**

[a] *Institute of Chemistry and Chemical Technology, Krasnoyarsk Scientific Center, Siberian Branch, Russian Academy of Sciences, Krasnoyarsk, 660036 Russia*

[b] *Kirensky Institute of Physics, Krasnoyarsk Scientific Center, Siberian Branch, Russian Academy of Sciences, Krasnoyarsk, 660036 Russia*

[c] *Boreskov Institute of Catalysis, Siberian Branch, Russian Academy of Sciences, Novosibirsk, 630090 Russia*

**e-mail: 4ubekpam@mail.ru*

Received December 7, 2019; revised December 7, 2019; accepted January 22, 2020

**Abstract**—A composite based on ultra-high-molecular-weight polyethylene (UHMWPE) added with 1 wt % of multiwalled carbon nanotubes (MWCNTs) with a high permittivity ($\varepsilon = 4.5$) and a low dielectric loss ($\tan\delta = 10^{-2}$) in the frequency range from 100 Hz to 100 MHz has been synthesized, and its main mechanical characteristics have been studied. The material has a low (22 MPa) breaking strength, a high (700%) tensile elongation, and an abrasion resistance higher than that of pure UHMWPE by 37%. It is shown using the X-ray diffraction and differential scanning calorimetry data that the changes in the mechanical properties of the composite are related to the changes in the polymer matrix structure under the action of the high-intensity ultrasonic radiation used for embedding MWCNTs into the polymer.

**DOI:** 10.1134/S1063784220070129

## 1. INTRODUCTION

There is a trend in modern engineering and technology to transition from conventional materials to polymers and polymer-based composites, which can withstand extreme operation conditions (low temperatures, exposure to aggressive media, high humidity, deformation loads, etc.). Such materials include ultra-high-molecular-weight polyethylene (UHMWPE) characterized by high wear, impact, and corrosion resistance and a wide operating temperature range, from cryogenic temperatures to 100°C. This polymer is widely used in various fields of engineering and medicine [1–5]. Its global production is steadily increasing, and so even a minor improvement in its properties will inevitably extend the range of its application. The improvement of the strength characteristics of UHMWPE is a very challenging task. It is conventionally solved by embedding various fillers (carbon nanotubes, graphenes, ceramic particles, etc.) into polyethylene [6–8], which sometimes make it possible to enhance the polymer ultimate strength by a factor of more than 5. Embedding of abrasive particles increases the abrasion resistance by a factor of 2–150 [9–11].

One important feature of UHMWPE is its radio transparency in the microwave range caused by a dielectric loss of about $10^{-4}$. UHMWPE is promising, in particular, for the creation of radomes for protection of radar equipment from climatic and environmental factors (impacts and aggressive media) and as a material for microwave filter or dielectric resonator substrates. For this purpose, the polymer should have a high permittivity ($\varepsilon > 5$), a low dielectric loss ($\tan\delta < 10^{-3}$) in the microwave range, and high mechanical characteristics (strength, wear resistance, impact number, etc.). Meanwhile, the permittivity of pure UHMWPE is 2.3.

The permittivity of a polymer can be increased by embedding a high-permittivity ceramic phase in high concentrations [12–14]. However, this inevitably degrades the mechanical properties of a material and increases the weight of a product [15, 16]. The permittivity of UHMWPE can be increased by embedding conducting carbon nanotubes (CNTs), as has been done for polymers of other types [17, 18]. In this case, the dielectric loss can be maintained at a level of about $10^{-3}$ [19]. According to the Maxwell–Wagner polarization theory, to ensure the most effective permittivity growth at the maintained low dielectric loss, CNTs

must be uniformly distributed over the polymer matrix in the form of fine submicron clusters and individual nanoparticles isolated from each other by a polymer.

In addition, it should be noted that embedding of nanotubes can improve the strength properties of UHMWPE [20–22]. In the opinion of the authors of [23], a necessary condition for improving the strength properties of a polymer composite is not only the strong interfacial interaction between the matrix and nanotubes, but also the uniform distribution of CNTs in the bulk of a polymer. Otherwise, CNT clusters will concentrate stresses, which degrade the properties of the material.

To date, the UHMWPE–CNT composites characterized by the high electrical conductivity and strength characteristics have been studied in sufficient detail [20–22, 24–33]. However, no works reporting on the successful fabrication and study of the UHMWPE–CNT composite, which combines the high mechanical properties, high permittivity, and low dielectric loss, have been published yet. To obtain such a material, a synthesis method is required that would ensure the uniform CNT distribution in the UHMWPE matrix. Among the available techniques for synthesizing composites based on UHMWPE with nanoparticle inclusions, the most universal and effective one is component mixing in a solution. This synthesis technique allows one to obtain composites with a tuned filler distribution uniformity [34] due to the flexible control of the synthesis conditions (temperature, time, liquid medium, mixing method, sequence of operations, etc.). The right choice of the filler concentration and synthesis regime will provide the optimal distribution of CNTs in the polymer matrix with a combination of high mechanical properties and desired electrophysical characteristics of the composite in the microwave range.

The aim of this study is to synthesize a UHMWPE composite modified with multiwalled carbon nanotubes (MWCNTs) with high permittivity and low dielectric loss in a wide (from 100 Hz to 100 MHz) frequency range and investigate its main mechanical characteristics. The UHMWPE composites were fabricated by mixing the components in a solution of an organic solvent using the high-intensity ultrasonic treatment.

## 2. EXPERIMENTAL

In this work, we used Braskem UHMWPE with a molecular weight of $6.4 \times 10^6$ g/mol and an average powder particle size of 150 μm and MWCNTs with an average diameter of 7 nm, a length of 2–2.5 μm, and an electrical conductivity of 2500 Sm $m^{-1}$ synthesized at the Boreskov Institute of Catalysis, Siberian Branch, Russian Academy of Sciences (Novosibirsk) [35].

The UHMWPE-based composites with the MWCNT addition were obtained by mixing the components in a solution of an organic solvent using ultrasonic treatment. Based on a previous study [36], we selected optimal synthesis regimes to ensure the most uniform filler distribution over the polymer matrix. To obtain the composites, MWCNTs were treated in xylene by ultrasound (US) with an intensity of no lower than 100 W/$cm^2$ for 20 min before the formation of a homogeneous suspension. Then, the MWCNT suspension was added with the UHMWPE powder and the mixture was subjected to the ultrasonic treatment with an intensity of no lower than 100 W/$cm^2$ for 20 min at a temperature of 130°C; this yielded a homogeneous xylene solution of the polymer and MWCNTs. After filtration, the precipitate was dried in vacuum for 48 h at a temperature of 90°C. The MWCNT concentrations in the composite were 1, 4, and 8 wt %. The electrical characteristics of the composites were investigated, the material with the high permittivity and the lowest dielectric loss was selected among them, and its mechanical properties (the ultimate strength, yield point, modulus of tensile elasticity, and wear resistance) were studied.

To establish the effect of the ultrasonic treatment on the mechanical properties of the polymer composite, an additional UHMWPE sample without MWCNTs was synthesized by the above-described technique: the UHMWPE powder in xylol was subjected to ultrasonic treatment with an intensity of no lower than 100 W/$cm^2$ for 20 min at a temperature of 130°C, which yielded a homogeneous polymer solution. After filtering, the precipitate was dried in vacuum for 48 h at a temperature of 90°C; the obtained sample was designated UHMWPE-UZ.

The experimental samples were prepared by hot pressing at a pressure of 6 MPa and a temperature of 160°C.

The complex conductivity and complex permittivity of the composites were studied in the frequency range from 100 Hz to 100 MHz using the impedance measurements with an Agilent Technology E5061B vector network analyzer. The impedance spectroscopy method consists in the measurement of the ac electric current flowing through the investigated materials and determination of the dispersion of the total complex impedance (impedance absolute value $|Z|$) and phase φ. Then, real impedance component $Z'(f) = |Z|\cos\varphi$ and imaginary impedance component $Z''(f) = |Z|\sin\varphi$ are calculated. To measure impedance $|Z|$ and phase φ, thin indium electrodes with a negligible transient resistance were pressed to the end surfaces of the composite samples. The samples under study were disk-shaped with a diameter of 16 mm and a thickness of 1 mm.

The components of the complex permittivity and conductivity were calculated using the formulas [37]

$$\varepsilon'_{\text{eff}} = \frac{-Z''}{\omega C_0(Z'^2 + Z''^2)}, \quad \varepsilon''_{\text{eff}} = \frac{-Z'}{\omega C_0(Z'^2 + Z''^2)}, \quad (1)$$

$$\sigma' = Y'\frac{d}{S}, \quad \sigma'' = Y''\frac{d}{S}, \tag{2}$$

where $\omega$ is the circular frequency; $C_0$, $d$, and $S$ are the geometric capacitance, and thickness and area of the measuring cell plates; and $Y'$ and $Y''$ are the real and imaginary components of the admittance.

The tensile strength characteristics of the material (the ultimate strength, yield point, and modulus of elasticity) were measured on an Inspekt Table Blue 5kN facility (Hegewald & Peschke, Germany). The tensile speed was 500 mm/min. The investigated samples had the form of strips 60 × 3 × 2 mm in size. At least three measurements were performed for each type of material and the results were averaged.

The composites were tested for the abrasion resistance upon sliding along a renewable surface using an MZ-4060 tester according to GOST (State Standard) 23509-79. A coated abrasive with a grain size of 160–200 μm was used. The normal force pressing the sample to a drum was 10 N. The mass loss of the experimental sample was calculated from the difference between its masses before and after the abrasion test. The samples investigated for abrasion were weighed accurate to ±1 mg. Abrasion $\Delta$ of the composites was determined by the formula

$$\Delta = \frac{(m_1 - m_2)}{m_1} \times 100\%, \tag{3}$$

where $m_1$ is the mass loss of pure UHMWPE and $m_2$ is the mass loss during abrasion of the composite. The $\Delta$ value is a percentage of a decrease in the mass loss for the investigated material during abrasion as compared with the initial UHMWPE. To determine the abrasive ability of the coated abrasive, a control test was performed for the pure UHMWPE sample once every five tests. If the mass loss decreased by more than 10%, then the coated abrasive was replaced for a new one. The samples under study were 16 mm in diameter and 6 mm thick.

The sample surface after the abrasion test was studied on a Hitachi TM3000 Benchtop scanning electron microscope (Japan).

Differential scanning calorimetry (DSC) of the investigated samples was performed on a Netzsch 204 F1 Phoenix device (Germany) by the ASTM D3418-15 technique in argon atmosphere at a flow rate of 30 mL/min in closed aluminum crucibles with a volume of 25 μL. The samples were shot according to the melting–crystallization–melting program in the temperature range from 25 to 160°C at a rate of 10°C/min. The melting temperature and enthalpy were determined from the second melting data. Degree of crystallinity $X$ of polyethylene was calculated by the formula

$$X = \frac{\Delta H_m}{\Delta H_0} \times 100\%, \tag{4}$$

where $\Delta H_m$ is the sample melting enthalpy calculated from the area under the endothermic melting peak and $\Delta H_m = 290$ J/g is the melting enthalpy of the polymer with a crystallinity of 100% [38].

The structure of the material samples was studied using X-ray diffraction (XRD) analysis at station no. 2 Precision Diffractometry and Anomalous Scattering of the Siberian Synchrotron and Terahertz Radiation Center (SSTRC). The measurements were performed in the Bragg–Brentano geometry using a weakly diverging X-ray beam and a crystal analyzer to exclude the peak broadening and displacements caused by the sample geometry. Due to the small size of the investigated area, the exposure time was chosen to be 15 s. The X-ray wavelength was 0.154 nm, and the scanning step was 0.02°.

## 3. RESULTS AND DISCUSSION

In this work, we determined, first of all, the impedance dispersion for the investigated materials and, using formulas (1), calculated the permittivity as a function of frequency in order to find a dielectric sample of the composite with the high permittivity and low dielectric loss.

Figure 1 shows the frequency dependences of the real component of complex permittivity $\varepsilon'$ and dissipation factor $\tan\delta$ of the UHMWPE composites with different MWCNT contents.

It can be seen that the permittivity and $\tan\delta$ values increase with the MWCNT concentration (Fig. 1). Moreover, the higher the filler concentration, the more pronounced the frequency dependence of the dielectric characteristics. The high $\varepsilon'$ and $\tan\delta$ values of the composites with MWCNT contents of 4 and 8% are explained by the polarization of coarse conducting MWCNT clusters according to the Maxwell–Wagner mechanism. In this case, in the sample with 8% of MWCNTs with a conductivity of $1.5 \times 10^2$ Sm m$^{-1}$, the MWCNT content obviously exceeds the percolation concentration; i.e., the sample has through conducting nanotube channels. This explains the huge values of the imaginary component of the permittivity and $\tan\delta$ at low frequencies.

The material containing 1% of MWCNTs has a permittivity higher than that of pure UHMWPE ($\varepsilon = 2.3$), which amounts to 4.5 and is almost frequency-independent in the range from 100 Hz to 100 MHz. In this case, the dissipation factor is low (about $10^{-2}$ (Fig. 1b)). The low-frequency conductivity of the composite with 1% of MWCNTs is $3 \times 10^{-9}$ Sm m$^{-1}$, which indicates the absence of a through network of conducting contacts in the material despite the high nanotube content. The high permittivity and low dielectric loss of this composite can be explained by the polarization of uniformly distributed noncontacting small clusters and individual MWCNTs under the action of an external electric field. This material, designated as

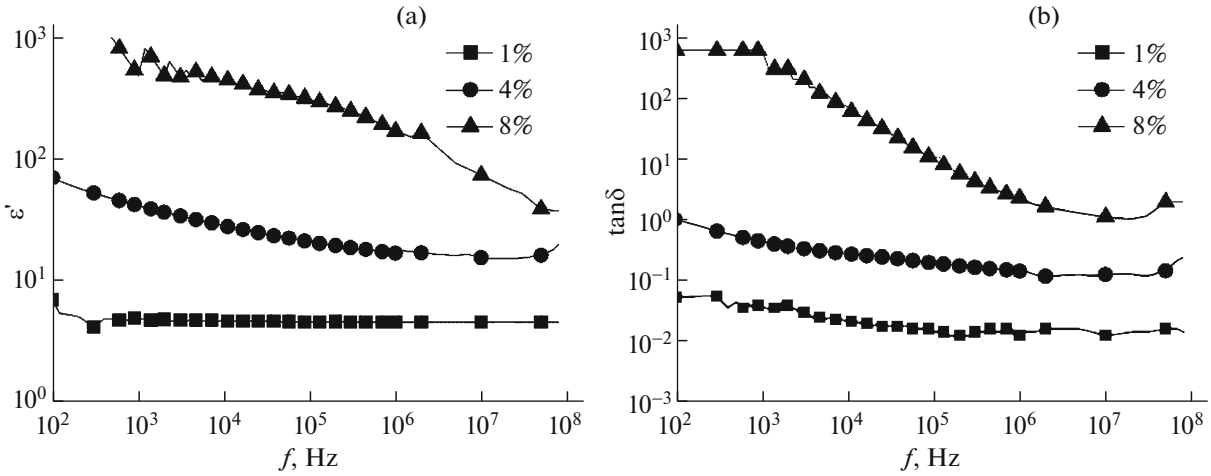


**Fig. 1.** Frequency dependences of the real part of the permittivity and dissipation factor of the composites: (a) $\varepsilon'(f)$ dependence and (b) $\tan\delta(f)$ dependence.

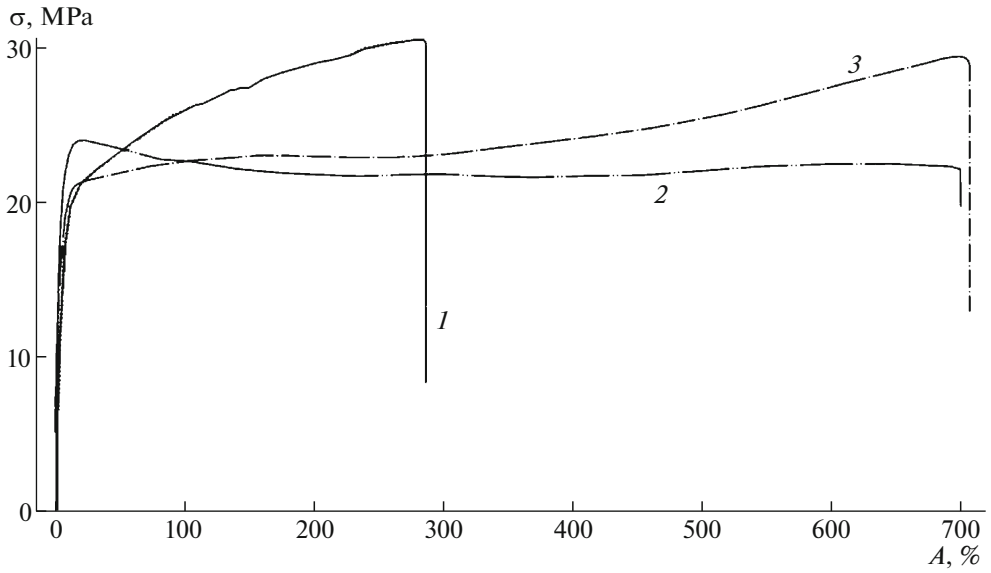


**Fig. 2.** Dependences of the conventional stress on the relative tensile elongation for (*1*) the initial UHMWPE, (*2*) UHMWPE–MWCNT 1% composite, and (*3*) UHMWPE–UZ material.

UHMWPE–MWCNT 1%, was selected for further investigations of the mechanical characteristics.

Figure 2 shows the curves plotted in coordinates of conventional stress σ and tensile elongation *A* obtained by extension of the initial UHMWPE, the dielectric composite containing 1% of MWCNTs, and the UHMWPE–UZ sample after the ultrasonic treatment of UHMWPE in xylene without MWCNTs.

It can be seen in Fig. 2 that the characteristics of the investigated materials under the extension significantly differ. The initial UHMWPE has a stress–strain diagram typical of this polyethylene with the elastic deformation and strain hardening areas characterized by an increase in the stress upon elongation. The initial UHMWPE has an ultimate strength of 30 MPa, a modulus of elasticity of 260 MPa, and a maximum breaking strain of 290%. The UHMWPE–MWCNT 1% and UHMWPE–UZ composites are characterized by high ductility (the maximum elongations are 700 and 710%, respectively) and high moduli of elasticity (310 and 300 MPa, respectively). The UHMWPE–UZ composite subjected to the UZ treatment without MWCNTs has the extended strain hardening region and preserves the ultimate strength of the initial polymer (29 MPa). In contrast, the UHMWPE–MWCNT 1% composite is characterized by a pronounced yield point at a stress of 24 MPa, after which

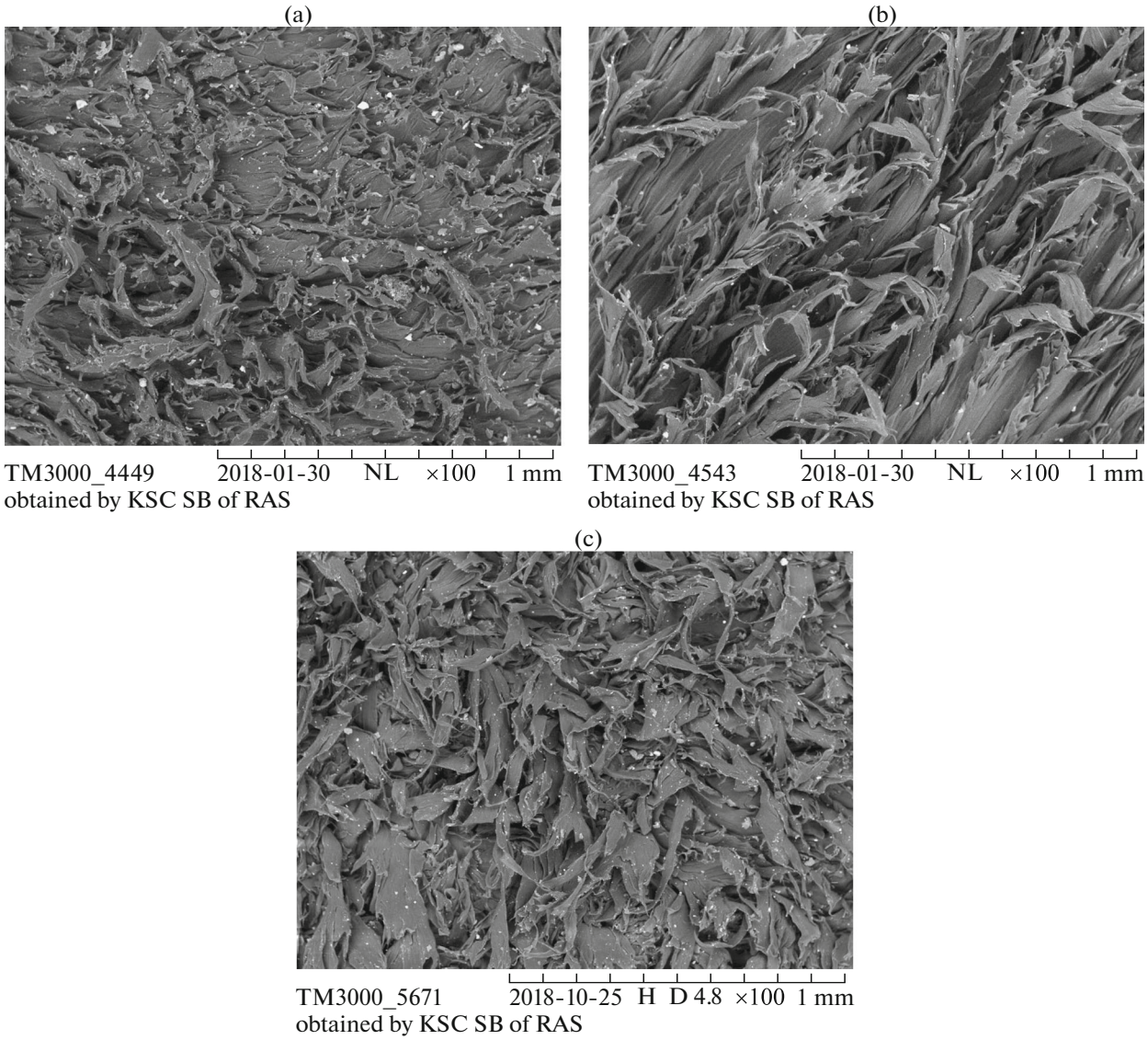


**Fig. 3.** Images of the sample surfaces after the abrasion test: (a) initial UHMWPE, (b) UHMWPE–MWCNT 1% composite, and (c) UHMWPE–UZ.

the strain decreases to 22 MPa and, then, the sample is strained at a constant stress up to its break.

According to the tests on the abrasion resistance upon sliding along a renewable surface, abrasion $\Delta$ of the UHMWPE–MWCNT 1% and UHMWPE–UZ materials calculated using Eq. (3) decreased by 37% as compared with the initial UHMWPE. In addition, we observed differences between the sample surface structures after the wear test (Fig. 3). The UHMWPE–MWCNT 1% and UHMWPE–UZ sample surfaces after the wear test had a pronounced fibrous structure.

To understand the origin of the differences between the mechanical characteristics of the investigated materials, they were examined by the DSC and XRD methods. The DSC curves of the investigated materials are shown in Fig. 4, where one can see the shifts of the melting peaks corresponding to the UHMWPE–MWCNT 1% and UHMWPE–UZ samples toward higher temperatures relative to the peak of the initial UHMWPE. The melting point of the initial UHMWPE sample is 139°C, and its degree of crystallinity is 46%. The UHMWPE–MWCNT 1% composite and the UHMWPE–UZ sample have the high melting point (142°C) and crystallinity (56%).

Figure 5 shows the X-ray diffraction patterns of the investigated materials, in which two highest reflections, (110) and (200), correspond to the orthorhombic modification of the UHMWPE matrix. The XRD analysis showed an increase in the degree of crystallinity from 70% for the initial UHMWPE to 80% for the UHMWPE–MWCNT 1% and UHMWPE–UZ materials, as well as an increase in the coherent scat-

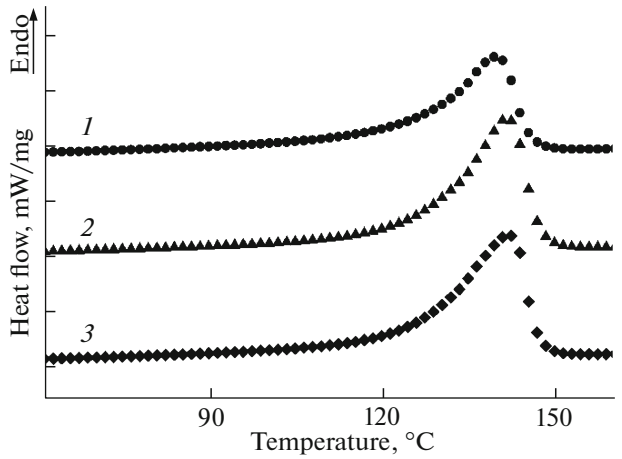


**Fig. 4.** DSC curves for (*1*) the initial UHMWPE, (*2*) UHMWPE–MWCNT 1% composite, and (*3*) UHMWPE–UZ samples.

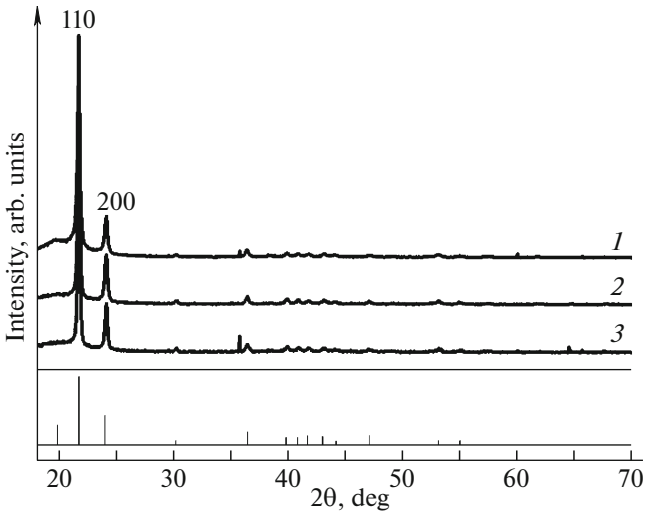


**Fig. 5.** X-ray diffraction patterns of (*1*) the initial UHMWPE, (*2*) UHMWPE–MWCNT 1% composite, and (*3*) UHMWPE–UZ samples.

tering regions from 35 nm for the initial UHMWPE to 43 nm for the UHMWPE–MWCNT 1% and UHMWPE–UZ materials. It is noteworthy that the degrees of crystallinity obtained by the DSC and XRD methods for the corresponding samples are strongly different. However, to eliminate the quantitative differences between the crystallinities determined by these two methods, additional investigations are needed. In this work, we pay attention to the fact that the DSC and XRD methods confirm an increase in the crystallinity of the UHMWPE–MWCNT 1% and UHMWPE–UZ samples by 10% relative to the initial UHMWPE.

According to the above-described DSC and XRD data, MWCNTs do not change the UHMWPE structure. Similar conclusions were drawn by the authors of study [39], in which the polyethylene-based composites with the MWCNT addition obtained by in situ polymerization were studied using the XRD technique. Thus, a factor determining the mechanical characteristics of the UHMWPE–MWCNT 1% composite is not the presence of nanotubes in it, but the effect of the ultrasonic treatment included in the process of its preparation. The effect of ultrasound on the UHMWPE solution at high temperature (130°C) apparently leads to the violation of van der Waals bonds between individual polymer chains distributed in the solvent in the form of individual chains or weakly bound clusters. Upon cooling the solution, free polymer chains form energetically favorable crystalline phases with a lower potential energy, which was detected by the DSC and XRD methods. In this case, the size of structural formations increases, which apparently leads to a corresponding increase in the moduli of elasticity of the materials. It can be supposed that the amorphous polymer phase is less entangled than that of the initial UHMWPE, which explains the growth of the ductility of the materials synthesized at 130°C. The increase in the wear resistance can also be explained by a decrease in the entanglement of polymer chains in the material, which weakens the ability of particles of the coated abrasive used in the abrasion test to tear out the sample fragments. As a result, the material surface after the abrasive action acquires a fibrous texture (Figs. 3b, 3c), in contrast to the outworn surface of pure UHMWPE (Fig. 3a). Embedding of MWCNTs into UHMWPE at a mixing temperature of 130°C reduces the tensile strength of polyethylene (Fig. 2). There is apparently no reliable coupling between UHMWPE and MWCNTs, which, in this case, are defects distributed over the polymer matrix.

## 4. CONCLUSIONS

Using the component mixing in the solution at a temperature of 130°C with the ultrasonic treatment, a UHMWPE-based composite supplemented with 1 wt % of MWCNTs was obtained, which has a high permittivity (4.5) and low dielectric loss (about $10^{-2}$) that is almost frequency-independent in the measurement range from 100 Hz to 100 MHz. The composite is characterized by a yield point of 24 MPa, a breaking strength of 22 MPa, and a huge (700%) elongation. The abrasion resistance is higher than that of pure UHMWPE by 37%. It was shown that embedding of MWCNTs into UHMWPE by mixing with the use of the ultrasonic treatment at a temperature of 130°C changes the mechanical properties of polyethylene due to the ultrasonic treatment of the polymer solution rather than due to the introduction of nanotubes and, as a result, a different polymer microstructure with the high degree of crystallinity forms upon cooling.

## ACKNOWLEDGMENTS

The authors are grateful to M.A. Mats'ko, Cand. Chem. Sci., head of the laboratory of the Boreskov Institute of Catalysis, Siberian Branch, Russian Academy of Sciences, and his colleagues for help in this work.

## CONFLICT OF INTEREST

The authors declare that they have no conflicts of interest.

## REFERENCES

1. H. van der Werff and U. Heisserer, in *Advanced Fibrous Composite Mater. Ballistic Protect*, Ed. by X. Chen (Elsevier, 2016), Chap. 3, pp. 71–108. https://doi.org/10.1016/B978-1-78242-461-1.00003-0
2. R. Marissen, Mater. Sci. Appl. **2** (5), 319 (2011). https://doi.org/10.4236/msa.2011.25042
3. W. Li, D. Xiong, X. Zhao, L. Sun, and J. Liu, Mater. Des. **102**, 162 (2016). https://doi.org/10.1016/j.matdes.2016.04.006
4. K. Karthikeyan and B. P. Russell, Mater. Des. **63**, 115 (2014). https://doi.org/10.1016/j.matdes.2014.05.069
5. F. Ansaria, B. Gludovatz, A. Kozak, R. O. Ritchie, and L. A. Pruitt, J. Mech. Behav. Biomed. Mater. **60**, 267 (2016). https://doi.org/10.1016/j.jmbbm.2016.02.014
6. A. V. Maksimkin, F. S. Senatov, V. D. Danilov, K. S. Mostovaya, S. D. Kaloshkin, M. V. Gorshenkov, A. P. Kharitonov, and D. I. Chukov, Mendeleev Commun. **26** (4), 350 (2016). https://doi.org/10.1016/j.mencom.2016.07.028
7. F. S. Senatov, A. N. Kopylov, N. Yu. Anisimova, M. V. Kiselevsky, and A. V. Maksimkin, Mater. Sci. Eng., C **48**, 566 (2015). https://doi.org/10.1016/j.msec.2014.12.050
8. J. C. Baena, J. Wu, and Z. Peng, Lubricants **3** (2), 413 (2015). https://doi.org/10.3390/lubricants3020413
9. K. Plumlee and C. J. Schwartz, Wear **267** (5–8), 710 (2009). https://doi.org/10.1016/j.wear.2008.11.028
10. D. S. Xiong, J. M. Lin, and D. L. Fan, Biomed. Mater. **1** (3), 175 (2006). https://doi.org/10.1088/1748-6041/1/3/013
11. G. E. Selyutin, Yu. Yu. Gavrilov, O. E. Popova, E. N. Voskresenskaya, V. A. Poluboyarov, V. A. Voroshilov, and A. V. Turushev, RF Patent No. RU 2 381 242 C2, Byull. Izobret., No. 4 (2010).
12. M. T. Sebastian, S. Thomas, and S. George, *Appl. Electromagnet. Conf. (AEMC), 2009*, pp. 1–4. https://doi.org/10.1109/AEMC.2009.5430628
13. Y. Kobayashi, T. Tanase, T. Tabata, T. Miwa, and M. Konno, J. Eur. Ceram. Soc. **28** (1), 117 (2008). https://doi.org/10.1016/j.jeurceramsoc.2007.05.007
14. S.-H. Xie, B.-K. Zhu, X.-Z. Wei, Z.-K. Xu, and Y.-Y. Xu, Composites, Part A **36** (8), 1152 (2005). https://doi.org/10.1016/j.compositesa.2004.12.010
15. K. M. Manu, S. Soni, V. R. K. Murthy, and M. T. Sebastian, J. Mater. Sci.: Mater. Electron. **24** (6), 2098 (2013). https://doi.org/10.1007/s10854-013-1064-y
16. J. Varghese, D. R. Nair, P. Mohanan, and M. T. Sebastian, Phys. Chem. Chem. Phys. **17**, 14943 (2015). https://doi.org/10.1039/c5cp01242b
17. J. Macutkevic, A. Paddubskaya, P. Kuzhir, J. Banys, S. Maksimenko, V. L. Kuznetsov, I. N. Mazov, and D. V. Krasnikov, J. Nanosci. Nanotechnol. **14** (7), 5430 (2014). https://doi.org/10.1166/jnn.2014.8705
18. Q. Li, Q. Xue, Q. Zheng, L. Hao, and X. Gao, Mater. Lett. **62** (26), 4229 (2008). https://doi.org/10.1016/j.matlet.2008.06.047
19. L. J. Romasanta, M. Hernandez, M. F. López-Manchado, and R. Verdejo, Nanoscale Res. Lett. **6**, 1 (2011). https://doi.org/10.1186/1556-276X-6-508
20. B. Meschi Amoli, S. A. Ahmad Ramazani, and H. Izadi, J. Appl. Polym. Sci. **125**, E453 (2012). https://doi.org/10.1002/app.36368
21. S. L. Ruan, P. Gao, X. G. Yang, and T. X. Yu, Polymer **44** (19), 5643 (2003). https://doi.org/10.1016/S0032-3861(03)00628-1
22. A. V. Maksimkin, S. D. Kaloshkin, M. S. Kaloshkina, M. V. Gorshenkov, V. V. Tcherdyntsev, K. S. Ergin, and I. V. Shchetinin, J. Alloys Compd. **536** (1), 538 (2012). https://doi.org/10.1016/j.jallcom.2012.01.151
23. P.-C. Ma, N. A. Siddiqui, G. Marom, and J.-K. Kim, Composites, Part A **41** (10), 1345 (2010). https://doi.org/10.1016/j.compositesa.2010.07.003
24. M. O. Lisunova, Ye. P. Mamunya, N. I. Lebovka, and A. V. Melezhyk, Eur. Polym. J. **43** (3), 949 (2007). https://doi.org/10.1016/j.eurpolymj.2006.12.015
25. A. Mierczynska, M. Mayne-L'Hermite, G. Boiteux, and J. K. Jeszka, J. Appl. Polym. Sci. **105** (1), 158 (2007). https://doi.org/10.1002/app.26044
26. H. Pang, C. Chen, Y. Bao, J. Chen, X. Ji, J. Lei, and Z.-M. Li, Mater. Lett. **79**, 96 (2012). https://doi.org/10.1016/j.matlet.2012.03.111
27. Y. Bin, A. Yamanaka, Q. Chen, Y. Xi, X. Jiang, and M. Matsuo, Polym. J. **39** (6), 598 (2007). https://doi.org/10.1295/polymj.PJ2006229
28. A. V. Eletskii, A. A. Knizhnik, B. V. Potapkin, and J. M. Kenny, Phys.-Usp. **58** (3), 209 (2015). https://doi.org/10.3367/UFNe.0185.201503a.0225
29. T. Deplancke, O. Lame, S. Barrau, K. Ravi, and F. Dalmas, Polymer **111**, 204 (2017). https://doi.org/10.1016/j.polymer.2017.01.040
30. A. V. Maksimkin, S. D. Kaloshkin, M. S. Kaloshkina, M. V. Gorshenkov, V. V. Tcherdyntsev, K. S. Ergin, and I. V. Shchetinin, J. Alloys Compd. **536**, S538 (2012). https://doi.org/10.1016/j.jallcom.2012.01.151
31. A. V. Maksimkin, K. S. Mostovaya, F. S. Senatov, D. I. Chukov, S. G. Nematulloev, and L. K. Olifirov, Results Phys. **7**, 1044 (2017). https://doi.org/10.1016/j.rinp.2017.02.024

32. S. R. Bakshi, J. E. Tercero, and A. Agarwal, Composites, Part A **38** (12), 2493 (2007). https://doi.org/10.1016/j.compositesa.2007.08.004

33. A. V. Maksimkin, A. P. Kharitonov, K. S. Mostovaya, S. D. Kaloshkin, M. V. Gorshenkov, F. S. Senatov, D. I. Chukov, and V. V. Tcherdyntsev, Composites, Part B **94**, 292 (2016). https://doi.org/10.1016/j.compositesb.2016.03.061

34. Y. A. Balogun and R. C. Buchanan, Composites Sci. Technol **70** (6), 892 (2010). https://doi.org/10.1016/j.compscitech.2010.01.009

35. I. Mazova, V. L. Kuznetsov, I. A. Simonova, A. I. Stadnichenko, A. V. Ishchenko, A. I. Romanenko, E. N. Tkachev, and O. B. Anikeeva, Appl. Surf. Sci. **258** (17), 6272 (2012). https://doi.org/10.1016/j.apsusc.2012.03.021

36. I. A. Markevich, G. E. Selyutin, N. A. Drokin, and B. A. Belyaev, Zh. Sib. Fed. Univ. Tekh. Tekhnol. **11** (2), 190 (2018). https://doi.org/10.17516/1999-494X-0022

37. D. K. Pradhan, R. N. P. Choudhary, and B. K. Samantaray, Int. J. Electrochem. Sci. **3**, 597 (2008).

38. S. K. Bhateja, S. M. Yarbrough, and E. H. Andrews, J. Macromol. Sci., Part B: Phys. **29** (1), 1 (1990). https://doi.org/10.1080/00222349008212332

39. M. A. Kazakova, A. G. Selyutin, N. V. Semikolenova, A. V. Ishchenko, S. I. Moseenkov, M. A. Matsko, V. A. Zakharov, and V. L. Kuznetsova, Composites Sci. Technol. **167** (20), 148 (2018). https://doi.org/10.1016/j.compscitech.2018.07.046

*Translated by E. Bondareva*